Protein Engineering, Design & Selection vol. 23 no. 4 pp. 261–269, 2010
Published online January 19, 2010 doi:10.1093/protein/gzp089

Isolation and characterization of an inhibitory human monoclonal antibody specific to the urokinase-type plasminogen activator, uPA

David Sgier[1], Kathrin Zuberbuehler[1], Stefanie Pfaffen[1] and Dario Neri[2]

[1]ETH Zürich HCI G396, Institute of Pharmaceutical Sciences, Department of Chemistry and Applied Biosciences, Wolfgang-Pauli-Strasse 10 CH-8093 Zürich, Switzerland

[2]To whom correspondence should be addressed.
E-mail: dario.neri@pharma.ethz.ch

Received December 11, 2009; revised December 11, 2009; accepted December 17, 2009

Edited by Philipp Holliger

The serine protease urokinase (uPA, urokinase-type plasminogen activator) is over-expressed in certain tumors and is considered to be the strongest single indicator of poor prognosis in patients with metastatic breast cancer. In this article, we describe the isolation and affinity maturation of a fully human recombinant antibody (termed DS2), specific to the human uPA and capable of inhibiting its enzymatic activity with an IC_{50} value in the low nanomolar range. The novel antibody cross-reacts with murine uPA. It was expressed both as scFv fragment and in IgG format, allowing a systematic comparative immunofluorescence (IF) analysis of the uPA expression patterns in a large panel of human und murine tumors and of normal human tissues. Although uPA was strongly expressed in virtually all tumor specimens tested, it exhibited only a weak expression in certain normal tissues (mainly in the colon, lung, spleen and bone marrow). IgG(DS2) was not able to inhibit cancer growth in immunocompromised mice bearing subcutaneous human MDA-MB-231 or DoHH-2 tumors. However, an *ex vivo* IF analysis confirmed the ability of the DS2 antibody to preferentially localize at the tumor site compared with normal organs. Collectively, these data suggest that uPA blocking antibodies may not be indicated for cancer growth inhibition strategies, but may serve as valuable tools for the implementation of pharmacodelivery strategies against a variety of different tumors.

Keywords: antibody phage technology/cancer/enzyme inhibition/immunofluorescence/uPA

Introduction

The use of monoclonal antibodies in cancer therapy continues to gain in importance, due to the ability of these molecules to concentrate therapeutic effects onto neoplastic lesions while sparing normal organs (Carter, 2006; Schrama *et al*., 2006; Weiner, 2006). Although originally monoclonal antibodies specific to membrane antigens on cancer cells have been used for tumor targeting applications, alternative targets such as markers of angiogenesis (Neri and Bicknell, 2005), stromal antigens (Hofheinz *et al*., 2003; Schliemann and Neri, 2007; Rybak *et al*., 2007) and intracellular proteins released at sites of necrosis (Miller *et al*., 1993; Street *et al*., 2006) are increasingly being considered. In this context, we and others have shown that the antibody-based targeting of enzymes, which are up-regulated at the tumor site, may represent an additional attractive avenue for therapeutic applications (Chrastina *et al*., 2003; Ahlskog *et al*., 2009a,b; Pfaffen *et al*., 2009).

The urokinase-type plasminogen activator (uPA) is a trypsin-like serine protease that can activate plasminogen into catalytically active plasmin. uPA exhibits only 54% similarity in amino acid sequence with the second endogenous plasminogen activator tPA (tissue-type plasminogen activator). While the main biological function of tPA seems to be associated with fibrinolysis, uPA is a central molecule in pericellular proteolysis and remodeling of the extracellular matrix (ECM; Carriero *et al*., 2009). uPA is produced as a single-chain pro-uPA that binds to a specific receptor (uPAR) on the surface of tumor and stromal cells. Upon binding to uPAR, pro-uPAR is converted to enzymatically active uPA mainly by plasmin. Active uPA in turn catalyzes plasminogen activation. Plasmin then activates a series of other proteases such as matrix metalloproteinases (MMPs), thereby triggering remodeling and degradation of the ECM.

uPA can also activate the precursor to the hepatocyte growth factor pro-HGF, which shows extensive homology with plasminogen, and the macrophage stimulating protein, thereby indirectly controlling cell proliferation, ECM invasion and prevention from apoptosis (van der Voort *et al*., 2000; Collen, 2001). Two endogenous uPA inhibitors, PAI-1 and PAI-2 (plasminogen inhibitor type 1 and 2), are known to inhibit the enzyme. PAI-1 forms covalent complexes with uPA that are rapidly cleared by uPAR-dependent internalization, if the protease is receptor bound (Cubellis *et al*., 1990; Olson *et al*., 1992).

Several studies have established that uPA levels are elevated in certain tumors (Duffy, 1996; Sier *et al*., 1998). Importantly, high levels of uPA in extracts of primary breast carcinomas were reported to predict early relapse and poor prognosis (Duffy *et al*., 1998). This relationship was later confirmed with other cancer types (Duffy and Duggan, 2004). In the clinic, the two proteins such as uPA and PAI-1 are considered to be the strongest known prognostic indicators of shortened disease-free survival and overall survival in breast cancer and the most accurate predictors of metastasis in lymph-node negative tumors (Look *et al*., 2002; Lee *et al*., 2004). These data suggest that uPA may play a functional role in breast cancer progression, but the experimental evidence is still controversial. Experiments with cell cultures and animal models have indicated a biological role of uPA-catalyzed plasminogen activation in tumor progression (Dano *et al*., 1985; Andreasen *et al*., 1997). Studies

indicating decreased metastatic load in uPA-deficient mice ($uPA^{-/-}$ mice) support the idea that uPA activity contributes to local invasion and metastasis. However, primary lesions could still grow in the absence of this enzyme (Almholt *et al*., 2005).

The inhibition of the proteolytic activity of uPA for therapeutic purposes has so far mainly been addressed with small organic compounds. A number of low-molecular-weight uPA inhibitors are currently in clinical development, based on the observation of a reduced metastatic load in mouse models of breast cancer (Ke *et al*., 1997; Tamura *et al*., 2000; Schweinitz *et al*., 2004). Only a few polyclonal and monoclonal antibodies generated in mouse and rabbit have been described so far (Ossowski and Reich, 1983; Salerno *et al*., 1984; Petersen *et al*., 2001), but to our knowledge their performance in tumor inhibition or in pharmacodelivery experiments has not yet been reported. Furthermore, human monoclonal antibodies would be needed for applications in humans.

Antibody phage display technology has revolutionized the way human monoclonal antibodies are isolated (Winter *et al*., 1994). Typically, single-pot phage display libraries containing billions of different antibody clones are panned on a target antigen, immobilized on a suitable support, yielding good-quality binding specificities which can be used for a variety of applications (e.g. ELISA, immunoblotting, immunohistochemistry etc.; Nissim *et al*., 1994; Silacci *et al*., 2005). If appropriate, phage antibodies can be affinity matured by combinatorial mutagenesis and by panning the resulting libraries under stringent conditions (Winter *et al*., 1994; Pini *et al*., 1998; Silacci *et al*., 2006; Villa *et al*., 2008). Our laboratory has previously developed and validated large antibody phage display libraries, from which specific antibodies in scFv format can be isolated against a variety of different antigens (Pini *et al*., 1998; Silacci *et al*., 2005; Pfaffen *et al*., 2009). Additionally, many groups (including ours) have implemented technologies for the efficient conversion of scFv fragments into the full human IgG format (Zuberbuhler *et al*., 2009). Indeed, intact immunoglobulins may be a preferable format, due to their long circulatory half-life and to their ability to engage Fcγ receptors and activate the complement system.

Here, we describe the isolation, affinity maturation and characterization of a potent inhibitory human monoclonal antibody, specific to uPA. A comprehensive immunofluorescence (IF) analysis in healthy and cancer tissues revealed that uPA is strongly expressed in the majority of tumors tested, while being undetectable or only moderately expressed in normal tissues. The anti-uPA antibody was not able to inhibit tumor growth in mouse models, but exhibited an ability to preferentially localize at the tumor site following intravenous administration, thus making it a suitable candidate for antibody-based pharmacodelivery strategies.

Materials and methods

Cell lines

Cell culture media and supplements were purchased from Invitrogen (Basel, Switzerland).

The human glioblastoma cell line U87 (HTB-14, ATCC) was cultured in MEM medium, supplemented with 10% fetal calf serum (FCS) and antibiotic–antimycotic at 37°C and 5% CO_2. The murine teratocarcinoma cell line F9 (CRL-1720, ATCC) and the human breast adenocarcinoma cell line MDA-MB-231 (HTB-26D, ATCC) were cultured in DMEM containing 10% FCS and incubated at 37°C and 5% CO_2. The human ovarian cancer cell line SKOV-3 (HTB-77, ATCC) and the murine colon carcinoma cell line colon-38 were cultured in RPMI 1640 supplemented as described above. The human follicular lymphoma cell line DoHH-2 (DSMZ; Braunschweig, Germany) was maintained in log-phase growth in RPMI 1640 medium adjusted to contain 2 mM L-glutamine, 10 mM *N*-2-hydroxyethylpiperazine-*N*′-2-ethanesulfonic acid (HEPES), 1 mM sodium pyruvate, 4.5 g l^{-1} glucose, 1.5 g l^{-1} bicarbonate, 10% FCS and antibiotic–antimycotic at 37°C and 5% CO_2.

Selection of antibodies from the ETH-2-Gold library by phage display

Human monoclonal antibodies specific to uPA were isolated by biopanning from the ETH-2-Gold antibody phage display library (Silacci *et al*., 2005). Antibody selections were carried out on Immunotubes (Nunc, Roskilde, Denmark) coated with uPA (Accurate Chemicals, Westbury, NY, USA) at 54 μg ml^{-1} in PBS (20 mM NaH_2PO_4, 30 mM Na_2HPO_4, 100 mM NaCl, pH 7.4), as described previously (Silacci *et al*., 2005).

Bacterial supernatants containing recombinant antibody fragments were screened by ELISA as described previously (Viti *et al*., 2000). Clones with positive signal in ELISA were expressed in *E.coli* TG-1 and purified from culture supernatant by affinity chromatography using Protein A Sepharose Fast Flow resin (GE Healthcare, Otelfingen, Switzerland), as described previously (Silacci *et al*., 2005). Purified scFv format antibodies were analyzed by surface plasmon resonance (SPR) real-time interaction analysis on a high-density coated antigen-chip, using a BIAcore 3000 instrument (BIAcore AB, GE Healthcare).

Sequencing of scFv antibody genes

Antibodies were sequenced using Big Dye® Terminator V 3.1 Cycle Sequencing kit (Applied Biosystems, Foster City, CA, USA) on an ABI PRISM 3130 Genetic analyzer. Termination reactions were performed using primers Limb3long 5′-CAG GAA ACA GCT ATG ACC ATG ATT AC-3′ (annealing 110 bp upstream the scFv gene) and fdseq-long 5′-GAC GTT AGT AAA TGA ATT TTC TGT ATG AGG-3′ (annealing 100 bp downstream the scFv gene; Eurofins MWG Operon, Ebersberg, Germany).

Characterization of scFv antibody fragments

ScFv antibody fragments were expressed in *E.coli* and purified from culture supernatant by affinity chromatography using Protein A Sepharose Fast Flow Resin (GE Healthcare), as described previously (Silacci *et al*., 2005).

Purified antibodies were analyzed by SDS–PAGE and size exclusion chromatography on a Superdex 75 HR10/30 column (Amersham Biosciences, GE Healthcare), and the peak of the monomeric fraction was collected and used for affinity measurement by BIAcore on a low-density coated antigen chip.

Construction of affinity maturation libraries

Affinity maturation libraries were constructed by introducing sequence variability either in the CDR1 loops of heavy (VH) and light chain (VL) or in the CDR2 loops of VH and VL. Antibody residues are numbered according to Tomlinson *et al*. (1992). Mutations at positions 31, 31a, 32 (CDR1 of VL) and 31, 32, 33 (CDR1 of VH) or 50, 51, 52 (CDR2 of VL) and 52, 52a, 53 and 56 were introduced by PCR using partially degenerate primers (Eurofins MWG Operon) as described previously (Silacci *et al*., 2006; Villa *et al*., 2008).

Phage display selections were carried out as described above. Briefly, one single round of panning was performed on uPA immobilized on immunotubes (Nunc) at 10^{-7} M concentration which corresponds to a 10-fold reduced concentration compared with the initial selections. Bound phage was eluted with 100 mM triethylamine, as described in Silacci *et al*. (2005). Induced supernatants of individual clones were screened by ELISA and ranked by SPR analysis on a high-density coated antigen chip. The selections yielded the scFv format antibody DS2.

Cloning and expression of IgG(DS2)

The heavy and light chain of the human IgG1 format of DS2 were cloned as described in Zuberbuhler *et al*. (2009). Equimolar amounts of the recombinant vectors were used to cotransfect CHO-S cells (Gibco/Invitrogen, Basel, Switzerland) using Amaxa Nucleofactor (Amaxa AG, Cologne, Germany) following the manufacturer's protocol. Transfectomas were selected using 500 μg ml^{-1} of Geneticin (G418, Calbiochem, San Diego, CA, USA) and 250 μg ml^{-1} hygromycin B (Invitrogen). After 14 days of selection in RPMI medium supplemented with 10% FCS and selective antibiotics, cells were brought into suspension, and cultured in PowerCHO-CD 2 medium (Lonza, Vervier, Belgium).

Staining of recombinant CHO-S for secreted product and fluorescent-activated cell sorting FACS were performed as described earlier (Zuberbuhler *et al*., 2009). IgG(DS2) was purified from cell culture medium of monoclonal line by protein A affinity chromatography. The purified protein was analyzed by SDS–PAGE and size exclusion chromatography using a Superdex 200 HR 10/30 column.

Surface plasmon resonance (BIAcore)

Affinity measurements were performed on a BIAcore 3000 instrument. Antigen-coated chips were prepared by coupling antigen covalently to a CM5 sensor chip (BIAcore). For a high-density chip, low-density chip and ultra-low-density chip, 1000 RU of uPA, 300 RU and 100 RU, respectively, were immobilized per flow cell.

For the determination of the dissociation constants, the monomeric fraction of scFv(DS2) was collected by size-exclusion chromatography as described above. Serial 2-fold dilutions of the monomer were then used for real-time interaction analysis on the low-density chip at a flow rate of 20 μl min^{-1}. The kinetic constants k_{on}, k_{off} and K_D were evaluated using the BIAevaluation 4.1 software (BIAcore). In addition, the K_D value of the scFv(DS2) was determined by plotting the RU values at saturation against the concentration of the scFv antibody and fitting with the equation below:

$$RU = \frac{RU_{max}}{1 + K_D/c[\text{scFv}]} \quad (1)$$

The apparent affinity of the IgG(DS2) was analyzed on an ultra-low-density chip using the BIAevaluation 4.1 software.

uPA inhibition assay

The inhibitory potentials of scFv(DS2) and IgG(DS2) were analyzed in a uPA inhibition assay as described by Scheuermann *et al*. (2008). Briefly, uPA (Accurate Chemicals) at 18.5 nM concentration was incubated with varying concentrations of the antibodies DS2 in 96-well microtiter plates (Nunc) for 15 min at room temperature. The reaction was started by addition of the fluorogenic substrate Z-RRG-AMC (Bachem, Bubendorf, Switzerland) dissolved in PBS to a final concentration of 0.1 mM in a total volume of 100 μl. The change in fluorescence signal (λ_{ex}: 383 nm; λ_{em}: 455 nm; cutoff filter: 420 nm) was recorded over 10 min using a SpectraMax microplate reader (Molecular Devices, Sunnyvale, CA, USA). The rate of fluorescence signal increase over time (dRFU/dt = reaction velocity v) was plotted against the corresponding inhibitor concentrations, and the IC_{50} value for the inhibitor was obtained by fitting to the equation below (KaleidaGraph V 4.0, Synergy Software):

$$v = \alpha \times 0.5 \times (-I_0 - E_0 + IC_{50} + ((I_0 - E_0 + IC_{50})^2 + 4 \times IC_{50} \times E_0)^{0.5}) \quad (2)$$

where $[I]_0$ is initial inhibitor concentration and $[E]_0$ is enzyme concentration.

IF on frozen tissue sections

Tumor tissue was embedded in cryoembedding medium (Microm, Volketswil, Switzerland), snap frozen in liquid nitrogen and stored at -80°C until sectioned. Tissue sections (10 μm) were fixed for 1 h in 4% paraformaldehyde (PFA), blocked with FCS and then stained for uPA. The IgG(DS2) was applied at 10 μg ml^{-1} and detected with goat anti-human IgG antibody (Sigma-Aldrich, St. Louis, MO, USA), followed by donkey anti-goat Alexa Fluor 594 antibody (Invitrogen). Nuclei were counterstained with 1 μg ml^{-1} DAPI (4′,6-diamidino-2-phenylindole; Invitrogen). All commercial reagents were diluted according to manufacturer's recommendation. Rinsing with PBS was performed in between all incubation steps. Finally, slides were mounted with Glycergel mounting medium (Dako, Glostrup, Denmark) and analyzed with a Zeiss Axioskop 2 mot fluorescence microscope (Carl Zeiss AG, Feldbach, Switzerland). Images were captured with an AxioCam MRC using AxioVision 4.7 image analysis software (Carl Zeiss AG).

The cross-reactivity of IgG(DS2) with normal tissue was studied on an FDA standard panel of healthy tissue (Biochain, Hayward, CA, USA). Sections were blocked with FCS and then incubated with 10 μg ml^{-1} of purified FITC-labeled IgG(DS2) for 1 h. For signal amplification, bound antibody was detected using rabbit anti-FITC antibody (MorphoSys, Oxford, UK) followed by Alexa Fluor 594 goat

anti-rabbit IgG (Invitrogen). Slides were analyzed as described above.

Immunocytochemistry/confocal laser scanning microscopy

Confocal laser scanning microscopy was done on formalin-fixed F9 cells grown on 4.2 cm^2 Falcon cell culture inserts (BD Biosciences, Allschwil, Switzerland) using the IgG(DS2) at 10 $\mu g\ ml^{-1}$. Binding was detected with a goat anti-human IgG antibody (Sigma-Aldrich), followed by donkey anti-goat Alexa Fluor 594 (Invitrogen). Nuclei were counterstained with 1 $\mu g\ ml^{-1}$ DAPI. Slices were mounted with mounting medium (70% (v/v) glycerol, 30 mmol l^{-1} Tris–HCl (pH 9.5), 5% (w/v) *n*-propyl-gallate (Sigma)) and analyzed with an LSM 510 META from Zeiss. Images were further processed using the IMARIS software (Bitplane AG, Zurich, Switzerland).

Tumor studies in mice. DoHH-2 lymphoma cells (1×10^7) were injected subcutaneously into the flank of 6- to 8-week-old female CB17/lcr SCID mice. MDA-MB-231 human breast carcinoma cells (2×10^6) were injected into the flank of 6- to 8-week-old female BALB/c nude mice. When tumors were established and clearly palpable (50–100 mm^3), mice were staged to maximize uniformity among the groups and injected into the lateral tail vein with either 200 μg IgG(DS2) (corresponding to a dosage of 10 mg antibody per kg of body weight), 200 μg human IgG isotype control (Cell Sciences, Canton, MA, USA), or control saline in a volume of 200 μl. All agents were injected weekly.

Mice were monitored daily, and tumor growth was measured three times per week with a digital caliper using the following formula: volume = length $\times$ width^2 $\times$ 0.5. Animals were killed when the tumor reached a volume of $>2000\ mm^3$.

All *in vivo* experiments were carried out according to Swiss regulations under a project license granted by the Veterinäramt des Kantons Zürich (169/2008).

Ex vivo fluorescence experiments. Two hundred micrograms of IgG(DS2) or an isotype control IgG antibody were injected intravenously into the lateral tail vein of mice bearing subcutaneously implanted murine F9 teratocarcinomas or human DoHH-2 follicular lymphomas. Animals were sacrificed 18 h after injection and tumors and normal organs (i.e. the heart, kidney, liver and lung) were excised, embedded in cryoembedding compound (Microm) and stored at $-80^{\circ}C$. Sections (10 μm) were cut and fixed with 4% PFA. For detection of injected IgG, goat anti-human IgG (Sigma-Aldrich) was applied, followed by donkey anti-goat Alexa Fluor 594 (Invitrogen). Endothelial cells were stained *ex vivo* with a rat anti-mouse CD31 antibody (BD Pharmingen, San Jose, CA, USA). Alexa Fluor 488 rabbit anti-rat IgG (Invitrogen) served as secondary antibody. Nuclei were counterstained with 1 $\mu g\ ml^{-1}$ DAPI (Invitrogen). All commercial reagents were diluted according to manufacturer's recommendation. Rinsing with PBS was performed in between all incubation steps. Slides were analyzed as described above.

Results

Antibody phage display selections against uPA

The human uPA was used for the isolation of human monoclonal antibodies from the ETH-2-Gold phage antibody library (Silacci *et al*., 2005). Clones from this library feature diversity in the CDR3 loops of the VH and VL domain. The library contains a single VH germline gene (DP47, which confers binding to Protein A (Hoogenboom and Winter, 1992)), while the VL domain is based either on a Vκ DPK-22 scaffold (Tomlinson *et al*., 1992) or on a Vλ DPL-16 scaffold (Tomlinson *et al*., 1992). Monoclonal antibodies in scFv format were isolated from the library by biopanning on immobilized antigen (Silacci *et al*., 2005) and showed specific binding in ELISA and SPR analyses. Selected clones were affinity matured by combinatorial mutagenesis of residues in the CDR1 and CDR2 loops of VH and VL domains, according to a procedure previously described by our group (Villa *et al*., 2008). This methodology yielded the human monoclonal antibody DS2 (Fig. 1), specific to human uPA and capable of cross-reacting with murine uPA (83% identity between the two proteins).

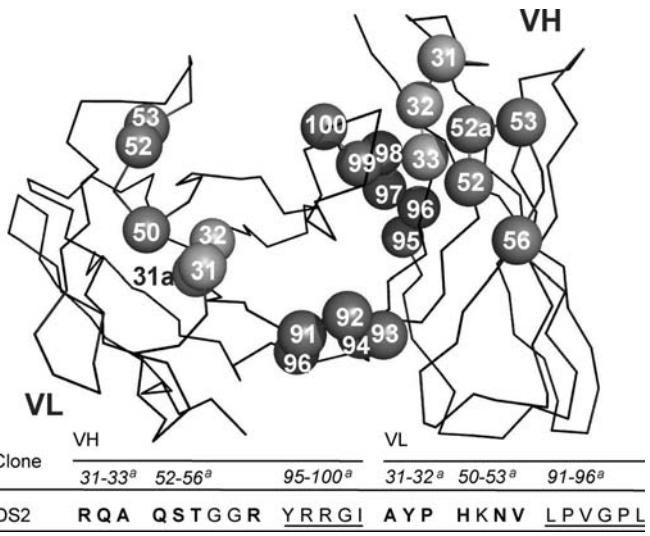

Fig. 1. ScFv antibody fragment structure, and relevant amino acid positions of the DS2 antibody. Positions that are mutated in the primary antibody library (ETH2-Gold) are underlined. Residues mutated during the affinity maturation process are in boldface. Single amino acid codes are used according to standard IUPAC nomenclature. [a]Numbering according to Tomlinson *et al*. (1992).

DS2 was expressed as scFv fragment in *E.coli* and purified from culture supernatant by protein A affinity chromatography, according to standard procedures (Silacci *et al*., 2005). In addition, the antibody was cloned and expressed as full human IgG (Zuberbuhler *et al*., 2009). The IgG was produced in CHO-S cells and purified from cell culture medium by protein A affinity chromatography, with non-optimized yields of 20 mg antibody per liter of culture from roller bottles. Both scFv and IgG antibody preparations were analyzed by SDS–PAGE and gel filtration (Fig. 2).

In vitro characterization of scFv(DS2) and IgG(DS2)

The dissociation constant of scFv(DS2) to human uPA was determined by BIAcore technology on a low-density microsensor chip, using the monomeric fraction of the scFv fragment isolated by size-exclusion chromatography. Figure 3a illustrates the BIAcore sensograms of scFv(DS2), which revealed a dissociation constant K_D of 6.4 nM [$k_{on} = 2.5 \times 10^5\ M^{-1}\ s^{-1}$ and $k_{off} = 1.5 \times 10^{-3}\ s^{-1}$]. This value is in line with the K_D value (=7.1 nM) obtained from the fitting of

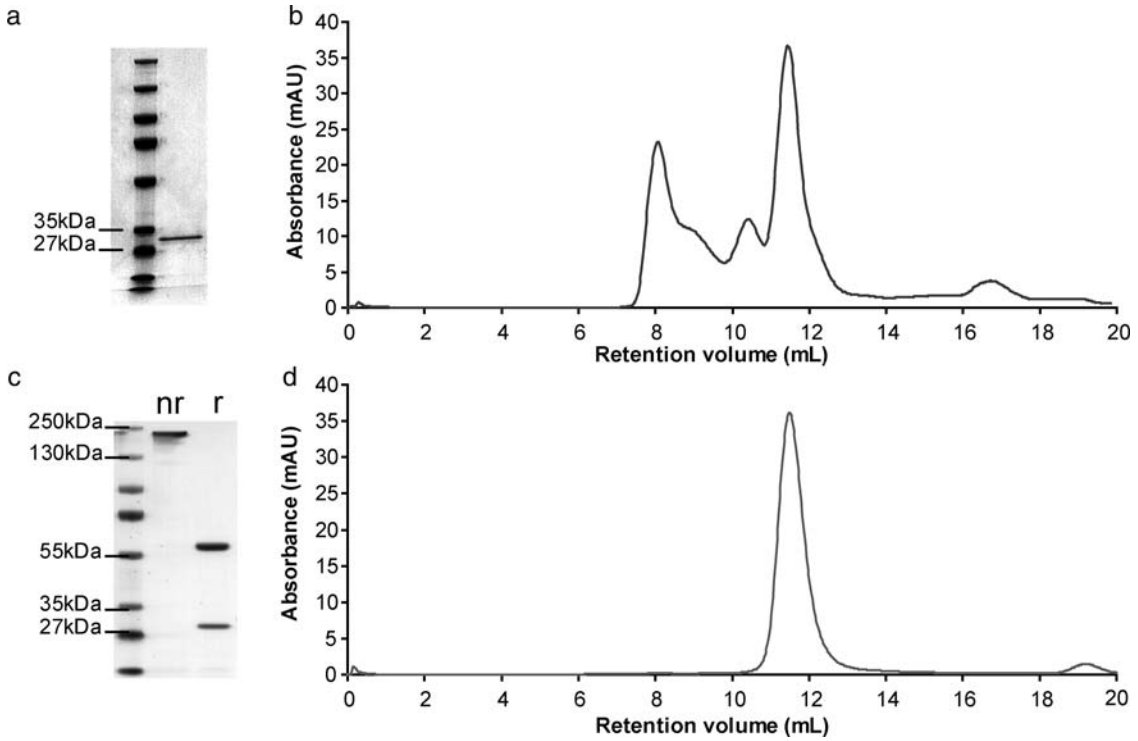

Fig. 2. Protein purification. SDS–PAGE analysis of the purified (**a**) scFv(DS2) and (**c**) IgG(DS2) under non-reducing (nr) and reducing (r) conditions. Size-exclusion chromatography of the purified (**b**) scFv(DS2) and (**d**) IgG(DS2) is also shown.

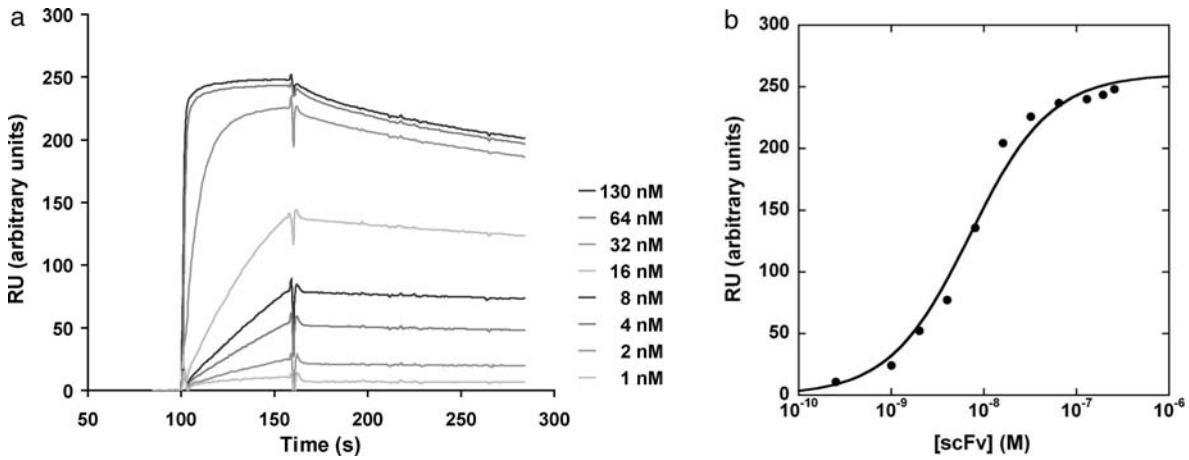

Fig. 3. BIAcore analysis of the purified monomeric scFv(DS2). The scFv antibody revealed a dissociation constant K_D of 6.4 nM (**a**). In addition, the affinity of scFv(DS2) was analyzed by plotting RU values at saturation against the different antibody concentrations (**b**). K_D value fitting with the KaleidaGraph V 4.0, Synergy Software revealed a K_D of 7.1 nM.

RU values at saturation against the scFv concentration (Fig. 3b).

Both scFv(DS2) and IgG(DS2) exhibited good selectivity for uPA over other trypsin-like enzymes as thrombin, Factor Xa, trypsin, chymotrypsin B, tPA and plasmin (Fig. 4). The antibodies recognized both the catalytically active two-chain uPA and the single-chain pro-uPA precursor.

Enzymatic inhibition

Both scFv(DS2) and IgG(DS2) were characterized in terms of their IC_{50} values for the inhibition of human uPA proteolytic activity. For scFv(DS2), an IC_{50} value of 6.7 nM was found. IgG(DS2) exhibited an IC_{50} value of 8.9 nM (Fig. 5). Both IC_{50} values are in line with the K_D values determined by BIAcore analysis.

IF analysis with IgG(DS2)

The recombinant antibody IgG(DS2) was extensively characterized by IF on cryosections of murine and human (xenograft) tumors and on healthy human tissues. In all tumors studied (human breast adenocarcinoma MDA-MB-231, human ovarian carcinoma SKOV-3, human B-cell lymphoma DoHH-2, human glioblastoma U87, murine F9 teratocarcinoma and murine colon-38 adenocarcinoma), a moderate to very strong staining could be observed. The strongest stainings were seen on MDA-MB-231 breast cancer, SKOV-3

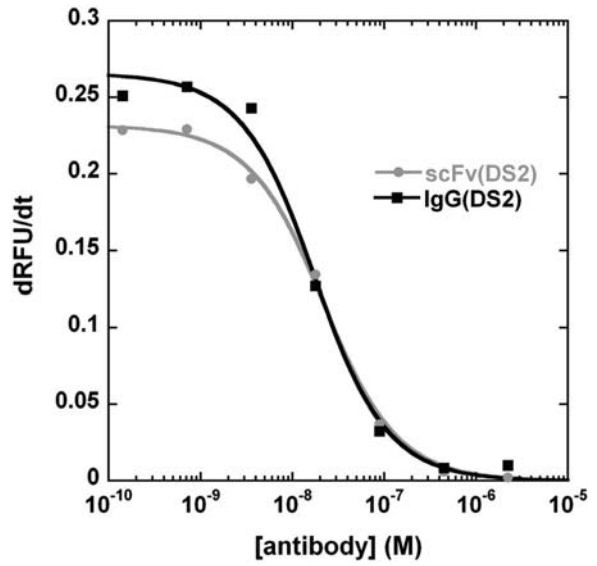

Fig. 4. Characterization of the inhibitory potential of the antibody DS2. The enzymatic activity of urokinase was measured in the presence of the antibodies scFv(DS2) and IgG(DS2) in varying concentrations. The reaction velocity, *v*, was plotted against the corresponding inhibitor concentrations, and the IC_{50} values of inhibitors were fitting with the KaleidaGraph V 4.0, Synergy Software.

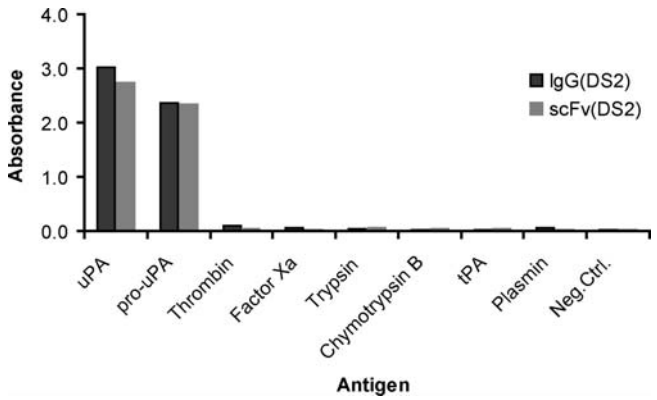

Fig. 5. Specificity of the uPA-binding antibodies. ELISA signals against other trypsin-like serine proteases. No antigen: wells only blocked with PBS, milk.

ovarian carcinoma and F9 teratocarcinoma (Fig. 6a). The staining performance of IgG(DS2) at the subcellular level was characterized by confocal laser scanning microscopic analysis on F9 cells, revealing expression in the cytoplasm and on the cell membrane (Fig. 6b).

The patterns of uPA expression in normal human tissue were studied on a FDA standard panel of health tissues (three donors per organ) using a frozen tissue array. uPA was undetectable in most tissues, while a moderate straining was observed in normal colon, lung, spleen, bone marrow and stomach (in one-thirds of donors only; Supplementary Figure S1 available at *PEDS* online).

Therapeutic activity of IgG(DS2) against localized tumor growth

To evaluate the therapeutic activity of IgG(DS2) in terms of primary tumor growth inhibition, mice bearing a subcutaneous MDA-MB-231 human breast adenocarcinoma or an

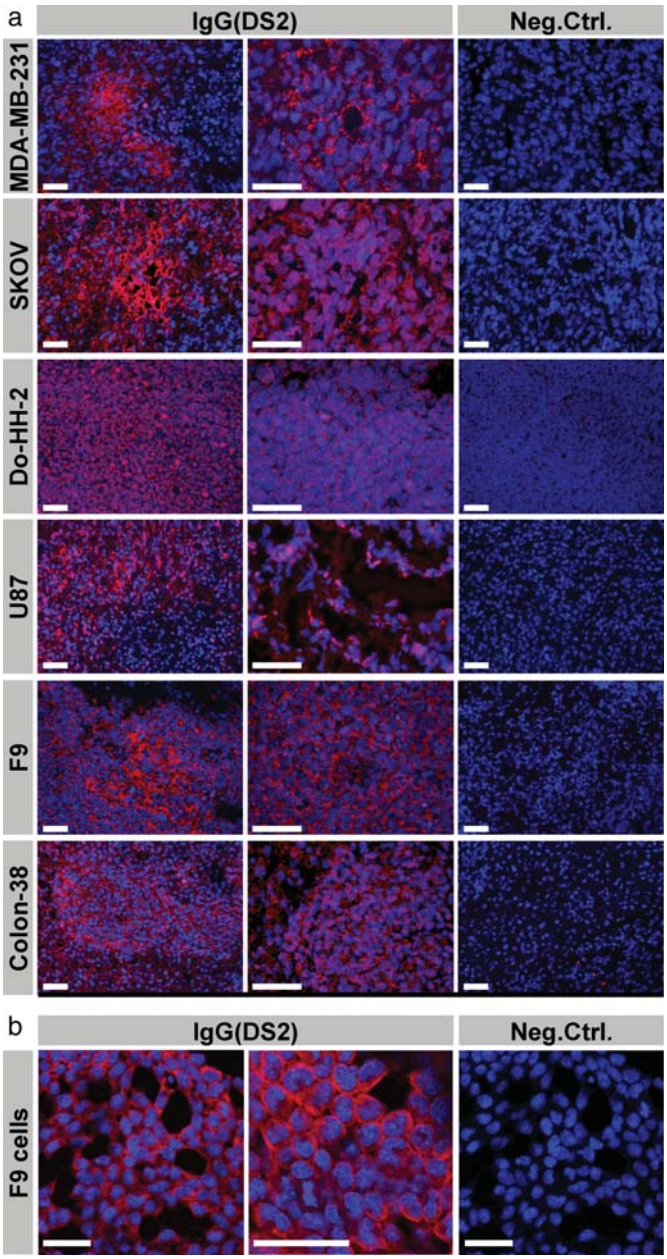

Fig. 6. Immunofluorescence analysis. IF performed on cryosections of murine and human (xenograft) tumors (**a**) (human breast adenocarcinoma MDA-MB-231, human ovarian carcinoma SKOV-3, human B-cell lymphoma Do-HH-2, human glioblastoma U87, murine F9 teratocarcinoma and murine colon-38 adenocarcinoma) (**b**). Characterization of subcellular expression of uPA in murine F9 teratocarcinoma cells. uPA was stained in red, whereas cell nuclei were stained in blue using DAPI. Scale bars represent 50 μm.

F9 murine teratocarcinoma were treated with weekly injections of either IgG(DS2) (200 μg), isotype control IgG or saline. No inhibition of primary tumor growth was observed (Fig. 7).

In vivo tumor targeting performance of IgG(DS2)

Mice bearing subcutaneous F9 or DoHH-2 tumors were injected intravenously with 200 μg of IgG(DS2) or of an isotype-matched monoclonal human antibody of irrelevant specificity in the experimental setting. After 18 h, mice were sacrificed and freshly frozen sections of tumors and healthy

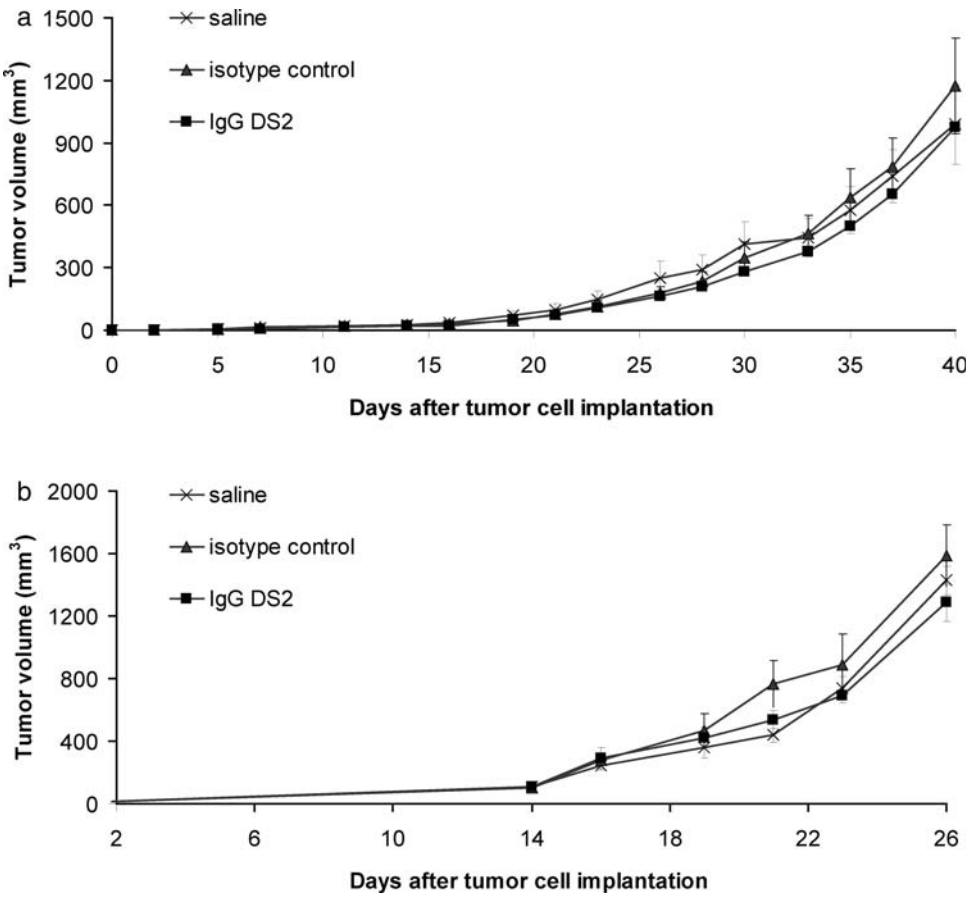

Fig. 7. Therapeutic activity of IgG(DS2) against primary tumor growth. Immunodeficient mice bearing subcutaneous MDA-MB-231 human breast adenocarcinomas (**a**) or DoHH-2 human follicular lymphomas (**b**) were treated with weekly injections (200 μg) of IgG(DS2) (filled square), human IgG isotype control (filled triangle) or saline (cross marks). Data represent mean tumor volumes (± SE).

organs were stained for human IgG (red), blood vessels (CD31 staining; green) and nuclei (DAPI staining; blue). A preferential uptake of IgG(DS2) in both tumors was observed. A weak staining of the liver for both specific and isotype-control antibodies could also be observed, compatible with liver recycling and hepatobiliary clearance of IgG molecules (Fig. 8). At these concentrations, IgG(DS2) reached structures distant from the tumor vasculature in both cancers. However, while the staining of tumor cells was homogenous in the DoHH-2 model, a heterogenous pattern of antibody uptake was observed for F9 tumors, in line with the *ex vivo* analysis of tumor sections (see also Fig. 6).

Discussion

In this article, we have described the isolation and affinity maturation of a human recombinant antibody against the serine protease uPA. The monoclonal antibody DS2 (in scFv and in IgG format) binds uPA with high affinity in the low nanomolar range without cross-reactivity to other serine proteases.

Urokinase activates plasminogen by cleavage of the Arg^{561}–Val^{562} bond in the catalytic domain of the zymogen (Andreasen *et al*., 2000). Our antibodies scFv(DS2) and IgG(DS2) were evaluated regarding their inhibitory potential in an *in vitro* enzyme assay using a synthetic fluorogenic peptide Z-Gly-Gly-Arg-AMC. Results with this assay were shown to correlate with those of the standard plasminogen activation assay (Zimmerman *et al*., 1978; Pierzchala *et al*., 1979). The antibodies DS2 exhibited IC_{50} values in the nanomolar range that closely matched the corresponding K_D value.

uPA has been implicated in tumor invasion and metastasis formation (Kim *et al*., 1998). Upregulation of uPA and its receptor in tumor tissue often correlates with increased malignancy and poor prognosis for patients with breast cancer and several other malignant tumors (Schmitt *et al*., 1997; Harbeck *et al*., 2002; Reuning *et al*., 2003). At present, only a few potent and selective uPA inhibitors have been developed, which could be used in animal models to evaluate the influence of the proteolytic activity of uPA on cancer metastasis and invasion (Tyndall *et al*., 2008; reviewed in Carriero *et al*., 2009).

It is recognized that membrane localization of uPA by interaction with the uPAR is of relevance to the enzymatic activity of uPA. In particular, kinetic studies have shown that receptor-bound uPA exhibits a considerably increased catalytic efficiency compared with the soluble protein (Ellis *et al*., 1991; Ploug *et al*., 2002). By SPR experiments with the uPAR (adapted from Kim *et al*., 2003), we could show that the antibody DS2 binds equally to soluble and receptor-bound uPA (data not shown) and does not influence the uPA–uPAR interaction. These observations are in line with the fact that IgG(DS2) targets tumor cells *in vivo* (Fig. 8).

When exploring the patterns of antigen expression in health and in cancer, it is important to consider data from the

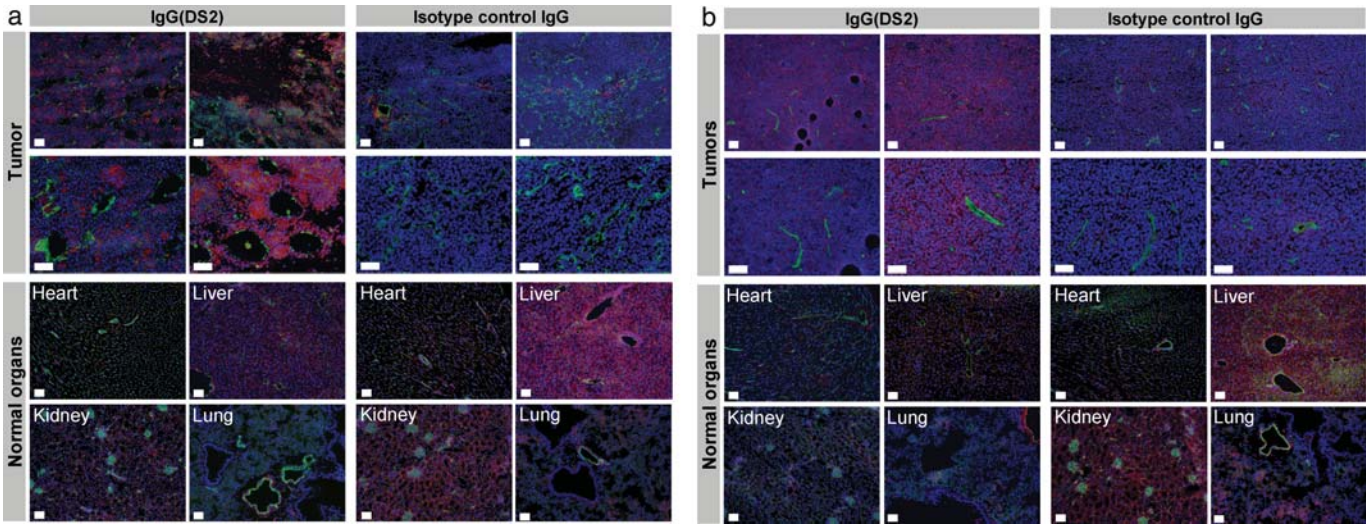

Fig. 8. *In vivo* localization experiments: *ex vivo* immunofluorescence. Mice bearing subcutaneous F9 murine teratocarcinomas (**a**) or DoHH-2 human follicular lymphomas (**b**) were injected with 200 μg of IgG(DS2) or isotype-matched control IgG. The figure shows microscopic images of tumor and organ sections 18 h after injection, confirming localization of IgG(DS2) at the site of tumor (red, injected IgG; green, *ex vivo* fluorescence staining of CD31; blue, nuclei). Scale bars represent 50 μm.

Human Protein Atlas (Berglund *et al*., 2008), a useful resource which compiles immunohistochemical data from commercial and custom-derived monoclonal and polyclonal antibodies. For these comparisons, it is important to consider that monoclonal antibodies of different affinity and epitope may sometimes yield contrasting staining results (Pfaffen *et al*., 2009). In our hands, the DS2 antibody exhibited a stronger staining of tumors compared with the data presented in the Human Protein Atlas. As for normal tissues, there was a general agreement, but we observed a moderate staining of certain normal tissues (e.g. lung, spleen and bone marrow), which had not previously been reported.

For many years, the research of our group has focused on the identification and validation of monoclonal antibodies with a pan-tumoral coverage potential. Even though certain markers of the sub-endothelial ECM (e.g. splice isoforms of tenascin-C, fibronectin and periostin) show a more restricted pattern of expression in normal tissues compared with DS2, the results presented in this article are still compatible with a possible role of anti-uPA antibodies for pharmacodelivery strategies (Carnemolla *et al*., 1996; Pini *et al*., 1998; Tarli *et al*., 1999; Viti *et al*., 1999; Borsi *et al*., 2002; Castellani *et al*., 2002; Neri and Bicknell, 2005; Berndorff *et al*., 2006; Brack *et al*., 2006; Tijink *et al*., 2006, Villa *et al*., 2008; Ahlskog *et al*., 2009a,b; Pedretti *et al*., 2009; Pfaffen *et al*., 2009; Schliemann *et al*., 2009a,b; Schwager *et al*., 2009). There is growing evidence that tumor-targeting monoclonal antibody derivatives (e.g. immunocytokines, radiolabeled antibodies, drug conjugates) may display tumor eradication potential both in animal models of cancer and in patients (Sauer *et al*., 2009; Schliemann *et al*., 2009a,b).

When injected at high doses, IgG(DS2) exhibited an impressive potential to homogenously reach tumor cells *in vivo*, including those not adjacent to vascular structures. Other reports from our group have shown that tumor antigens located hundreds of micrometers from the nearest blood vessels (e.g. carbonic anhydrase IX expressed at sites of hypoxia) can be targeted *in vivo* by cognate monoclonal antibodies (Ahlskog *et al*., 2009b). This contrasts with a previous study on the intravenous administration of Herceptin at high doses (10 mg/kg) in mice bearing F2-1282 tumors (Dennis *et al*., 2007), which evidenced a pattern of antibody uptake restricted to perivascular tumor cells. There is increasing evidence that antibody format, affinity, dose, patterns of antigen expression and vascular permeability of the individual tumor models may all contribute to the efficiency of *in vivo* antibody localization (Begent, 1999; Boerman *et al*., 2003; Adams *et al*., 2006; Ahlskog *et al*., 2009a; Schmidt and Wittrup, 2009).

To the best of our knowledge, most preclinical and clinical reports on pharmaceutical uPA inhibition strategies are based on low-molecular-weight inhibitors. High-affinity uPA blockers have been reported (Schweinitz *et al*., 2004), which allowed reduction of metastatic spread in animal models of tumor metastasis. Reduction of primary tumor growth was not reported so far. Additionally, off-target effects (i.e. undesired inhibition of other proteases or of other target proteins) may complicate the interpretation of preclinical therapy data.

In principle, monoclonal antibodies should represent the most selective avenue for validating the pharmaceutical potential of a putative tumor target. Impressive results on the inhibition of metastatic spread have been reported with uPA blockers (Schweinitz *et al*., 2004), which are in line with genetic data obtained in $uPA^{-/-}$ tumor-bearing mice (Almholt *et al*., 2005). In this article, we report that the potent uPA blocking antibody IgG(DS2) was not capable of inhibiting the growth of uPA-positive primary tumors. It is possible that the DS2 antibody may exhibit a therapeutic effect in preventing metastatic spread in animal models. However, in the clinical setting, patients often present with established bulky metastases and it is not clear whether the inhibition of new micrometastases may justify the development of a new pharmaceutical agent, to be combined with other regimens. The data presented in this article suggest a main role of uPA as a tumor-associated antigen for pharmacodelivery applications, rather than for the inhibition of proteolytic activity or for Fc-mediated anti-cancer strategies.

Supplementary data

Supplementary data are available at *PEDS* online.

Funding

This work was supported by the ETH Zürich (ETHIRA Grant), the Swiss National Science Foundation (grant # 3100A0-105919/1), the Swiss Cancer League (Robert-Wenner-Award), the SWISSBRIDGE and Stammbach Foundations, the European Union Projects IMMUNO-PDT (grant # LSHC-CT-2006-037489), DIANA (grant # LSHB-CT-2006-037681) and ADAMANT (HEALT-F2-2008-201342).

References

Adams,G.P., Tai,M.S., McCartney,J.E., Marks,J.D., Stafford,W.F., III, Houston,L.L., Huston,J.S. and Weiner,L.M. (2006) *Clin. Cancer Res.*, **12**, 1599–1605.

Ahlskog,J.K., Dumelin,C.E., Trussel,S., Marlind,J. and Neri,D. (2009a) *Bioorg. Med. Chem. Lett.*, **19**, 4851–4856.

Ahlskog,J.K., Schliemann,C., Marlind,J., Qureshi,U., Ammar,A., Pedley,R.B. and Neri,D. (2009b) *Br. J. Cancer*, **101**, 645–657.

Almholt,K., Lund,L.R., Rygaard,J., Nielsen,B.S., Dano,K., Romer,J. and Johnsen,M. (2005) *Int. J. Cancer*, **113**, 525–532.

Andreasen,P.A., Kjoller,L., Christensen,L. and Duffy,M.J. (1997) *Int. J. Cancer*, **72**, 1–22.

Andreasen,P.A., Egelund,R. and Petersen,H.H. (2000) *Cell Mol. Life Sci.*, **57**, 25–40.

Begent,R.H. (1999) *Br. J. Cancer*, **80**(Suppl. 1), 104–109.

Berglund,L., *et al*. (2008) *Mol. Cell Proteomics*, **7**, 2019–2027.

Berndorff,D., *et al*. (2006) *J. Nucl. Med.*, **47**, 1707–1716.

Boerman,O.C., van Schaijk,F.G., Oyen,W.J. and Corstens,F.H. (2003) *J. Nucl. Med.*, **44**, 400–411.

Borsi,L., Balza,E., Bestagno,M., Castellani,P., Carnemolla,B., Biro,A., Leprini,A., Sepulveda,J., Burrone,O. and Neri,D., *et al*. (2002) *Int. J. Cancer*, **102**, 75–85.

Brack,S.S., Silacci,M., Birchler,M. and Neri,D. (2006) *Clin. Cancer Res.*, **12**, 3200–3208.

Carnemolla,B., Neri,D., Castellani,P., Leprini,A., Neri,G., Pini,A., Winter,G. and Zardi,L. (1996) *Int. J. Cancer*, **68**, 397–405.

Carriero,M.V., *et al*. (2009) *Mol. Cancer Ther.*, **8**, 2708–2717.

Carter,P.J. (2006) *Nat. Rev. Immunol.*, **6**, 343–357.

Castellani,P., Borsi,L., Carnemolla,B., Biro,A., Dorcaratto,A., Viale,G.L., Neri,D. and Zardi,L. (2002) *Am. J. Pathol.*, **161**, 1695–1700.

Chrastina,A., Zavada,J., Parkkila,S., Kaluz,S., Kaluzova,M., Rajcani,J., Pastorek,J. and Pastorekova,S. (2003) *Int. J. Cancer*, **105**, 873–881.

Collen,D. (2001) *Hematol. Am. Soc. Hematol. Educ. Program.*, 1–9.

Cubellis,M.V., Wun,T.C. and Blasi,F. (1990) *EMBO J.*, **9**, 1079–1085.

Dano,K., Andreasen,P.A., Grondahl-Hansen,J., Kristensen,P., Nielsen,L.S. and Skriver,L. (1985) *Adv. Cancer Res.*, **44**, 139–266.

Dennis,M.S., Jin,H., Dugger,D., Yang,R., McFarland,L., Ogasawara,A., Williams,S., Cole,M.J., Ross,S. and Schwall,R. (2007) *Cancer Res.*, **67**, 254–261.

Duffy,M.J. (1996) *Clin. Cancer Res.*, **2**, 613–618.

Duffy,M.J. and Duggan,C. (2004) *Clin. Biochem.*, **37**, 541–548.

Duffy,M.J., Duggan,C., Mulcahy,H.E., McDermott,E.W. and O'Higgins,N.J. (1998) *Clin. Chem.*, **44**, 1177–1183.

Ellis,V., Behrendt,N. and Dano,K. (1991) *J. Biol. Chem.*, **266**, 12752–12758.

Harbeck,N., Kates,R.E., Look,M.P., Meijer-Van Gelder,M.E., Klijn,J.G., Kruger,A., Kiechle,M., Janicke,F., Schmitt,M. and Foekens,J.A. (2002) *Cancer Res.*, **62**, 4617–4622.

Hofheinz,R.D., *et al*. (2003) *Onkologie*, **26**, 44–48.

Hoogenboom,H.R. and Winter,G. (1992) *J. Mol. Biol.*, **227**, 381–388.

Ke,S.H., Coombs,G.S., Tachias,K., Corey,D.R. and Madison,E.L. (1997) *J. Biol. Chem.*, **272**, 20456–20462.

Kim,J., Yu,W., Kovalski,K. and Ossowski,L. (1998) *Cell*, **94**, 353–362.

Kim,K.S., Hong,Y.K., Lee,Y., Shin,J.Y., Chang,S.I., Chung,S.I. and Joe,Y.A. (2003) *Exp. Mol. Med.*, **35**, 578–585.

Lee,M., Fridman,R. and Mobashery,S. (2004) *Chem. Soc. Rev.*, **33**, 401–409.

Look,M.P., van Putten,W.L., Duffy,M.J., Harbeck,N., Christensen,I.J., Thomssen,C., Kates,R., Spyratos,F., Ferno,M. and Eppenberger-Castori,S., *et al*. (2002) *J. Natl Cancer Inst.*, **94**, 116–128.

Miller,G.K., Naeve,G.S., Gaffar,S.A. and Epstein,A.L. (1993) *Hybridoma*, **12**, 689–698.

Neri,D. and Bicknell,R. (2005) *Nat. Rev. Cancer*, **5**, 436–446.

Nissim,A., Hoogenboom,H.R., Tomlinson,I.M., Flynn,G., Midgley,C., Lane,D. and Winter,G. (1994) *EMBO J.*, **13**, 692–698.

Olson,D., Pollanen,J., Hoyer-Hansen,G., Ronne,E., Sakaguchi,K., Wun,T.C., Appella,E., Dano,K. and Blasi,F. (1992) *J. Biol. Chem.*, **267**, 9129–9133.

Ossowski,L. and Reich,E. (1983) *Cell*, **35**, 611–619.

Pedretti,M., Soltermann,A., Arni,S., Weder,W., Neri,D. and Hillinger,S. (2009) *Lung Cancer*, **64**, 28–33.

Petersen,H.H., Hansen,M., Schousboe,S.L. and Andreasen,P.A. (2001) *Eur. J. Biochem.*, **268**, 4430–4439.

Pfaffen,S., Hemmerle,T., Weber,M. and Neri,D. (2009) *Exp. Cell Res.*

Pierzchala,P.A., Dorn,C.P. and Zimmerman,M. (1979) *Biochem. J.*, **183**, 555–559.

Pini,A., Viti,F., Santucci,A., Carnemolla,B., Zardi,L., Neri,P. and Neri,D. (1998) *J. Biol. Chem.*, **273**, 21769–21776.

Ploug,M., Gardsvoll,H., Jorgensen,T.J., Lonborg Hansen,L. and Dano,K. (2002) *Biochem. Soc. Trans.*, **30**, 177–183.

Reuning,U., Magdolen,V., Hapke,S. and Schmitt,M. (2003) *Biol. Chem.*, **384**, 1119–1131.

Rybak,J.N., Trachsel,E., Scheuermann,J. and Neri,D. (2007) *ChemMedChem*, **2**, 22–40.

Salerno,G., Verde,P., Nolli,M.L., Corti,A., Szots,H., Meo,T., Johnson,J., Bullock,S., Cassani,G. and Blasi,F. (1984) *Proc. Natl Acad. Sci. USA*, **81**, 110–114.

Sauer,S., *et al*. (2009) *Blood*, **113**, 2265–2274.

Schliemann,C. and Neri,D. (2007) *Biochim. Biophys. Acta*, **1776**, 175–192.

Scheuermann,J., Dumelin,C.E., Melkko,S., Zhang,Y., Mannocci,L., Jaggi,M., Sobek,J. and Neri,D. (2008) *Bioconjug. Chem.*, **19**, 778–785.

Schliemann,C., Palumbo,A., Zuberbuhler,K., Villa,A., Kaspar,M., Trachsel,E., Klapper,W., Menssen,H.D. and Neri,D. (2009a) *Blood*, **113**, 2275–2283.

Schliemann,C., Roesli,C., Kamada,H., Borgia,B., Fugmann,T., Klapper,W. and Neri,D. (2009b) *Blood*.

Schmidt,M.M. and Wittrup,K.D. (2009) *Mol. Cancer Ther.*, **8**, 2861–2871.

Schmitt,M., Harbeck,N., Thomssen,C., Wilhelm,O., Magdolen,V., Reuning,U., Ulm,K., Hofler,H., Janicke,F. and Graeff,H. (1997) *Thromb. Haemost.*, **78**, 285–296.

Schrama,D., Reisfeld,R.A. and Becker,J.C. (2006) *Nat. Rev. Drug. Discov.*, **5**, 147–159.

Schwager,K., Kaspar,M., Bootz,F., Marcolongo,R., Paresce,E., Neri,D. and Trachsel,E. (2009) *Arthritis Res. Ther.*, **11**, R142.

Schweinitz,A., Steinmetzer,T., Banke,I.J., Arlt,M.J., Sturzebecher,A., Schuster,O., Geissler,A., Giersiefen,H., Zeslawska,E. and Jacob,U., *et al*. (2004) *J. Biol. Chem.*, **279**, 33613–33622.

Sier,C.F., *et al*. (1998) *Cancer Res.*, **58**, 1843–1849.

Silacci,M., Brack,S., Schirru,G., Marlind,J., Ettorre,A., Merlo,A., Viti,F. and Neri,D. (2005) *Proteomics*, **5**, 2340–2350.

Silacci,M., Brack,S.S., Spath,N., Buck,A., Hillinger,S., Arni,S., Weder,W., Zardi,L. and Neri,D. (2006) *Protein Eng. Des. Sel.*, **19**, 471–478.

Street,H.H., *et al*. (2006) *Cancer Biother. Radiopharm.*, **21**, 243–256.

Tamura,S.Y., *et al*. (2000) *Bioorg. Med. Chem. Lett.*, **10**, 983–987.

Tarli,L., Balza,E., Viti,F., Borsi,L., Castellani,P., Berndorff,D., Dinkelborg,L., Neri,D. and Zardi,L. (1999) *Blood*, **94**, 192–198.

Tijink,B.M., Neri,D., Leemans,C.R., Budde,M., Dinkelborg,L.M., Stigter-van Walsum,M., Zardi,L. and van Dongen,G.A. (2006) *J. Nucl. Med.*, **47**, 1127–1135.

Tomlinson,I.M., Walter,G., Marks,J.D., Llewelyn,M.B. and Winter,G. (1992) *J. Mol. Biol.*, **227**, 776–798.

Tyndall,J.D., Kelso,M.J., Clingan,P. and Ranson,M. (2008) *Recent Pat. Anticancer Drug Discov.*, **3**, 1–13.

van der Voort,R., Taher,T.E., Derksen,P.W., Spaargaren,M., van der Neut,R. and Pals,S.T. (2000) *Adv. Cancer Res.*, **79**, 39–90.

Villa,A., Trachsel,E., Kaspar,M., Schliemann,C., Sommavilla,R., Rybak,J.N., Rosli,C., Borsi,L. and Neri,D. (2008) *Int. J. Cancer*, **122**, 2405–2413.

Viti,F., Tarli,L., Giovannoni,L., Zardi,L. and Neri,D. (1999) *Cancer Res.*, **59**, 347–352.

Viti,F., Nilsson,F., Demartis,S., Huber,A. and Neri,D. (2000) *Methods Enzymol.*, **326**, 480–505.

Weiner,L.M. (2006) *J. Immunother.*, **29**, 1–9.

Winter,G., Griffiths,A.D., Hawkins,R.E. and Hoogenboom,H.R. (1994) *Annu. Rev. Immunol.*, **12**, 433–455.

Zimmerman,M., Quigley,J.P., Ashe,B., Dorn,C., Goldfarb,R. and Troll,W. (1978) *Proc. Natl Acad. Sci. USA*, **75**, 750–753.

Zuberbuhler,K., Palumbo,A., Bacci,C., Giovannoni,L., Sommavilla,R., Kaspar,M., Trachsel,E. and Neri,D. (2009) *Protein Eng. Des. Sel.*, **22**, 169–174.